Journal of Applied Polymer Science

Preparation and Characterization of Isotactic Polypropylene/High-Density Polyethylene/Carbon Black Conductive Films with Strain-Sensing Behavior

Shaodi Zheng, Shilin Huang, Danqi Ren, Wei Yang, Zhengying Liu, Mingbo Yang
College of Polymer Science and Engineering, State Key Laboratory of Polymer Materials Engineering, Sichuan University, Chengdu 610065, Sichuan, People's Republic of China
Correspondence to: Z. Liu (E-mail: liuzhying@scu.edu.cn)

ABSTRACT: Novel conductive films with a unique strain (ε)-sensing behavior and based on a blend of isotactic polypropylene (iPP), high-density polyethylene (HDPE), and carbon black (CB) were fabricated by an extrusion casting method. The morphology and ε-sensing behavior of the films were investigated. Scanning electron microscope images showed that the oriented lamellae with a growing direction perpendicular to the extrusion direction were obtained in the HDPE phase and were accompanied by a cocontinuous structure of the iPP phase and HDPE/CB phase. The conductive percolation threshold (m_c) and resistivity–ε behavior of the thin films are affected by the drawing ratio during the process of film preparation. The m_c and electrical resistance of the iPP/HDPE/CB composite films increased with the drawing ratio. The gauge factor of the films within the elastic region decreased with increasing drawing ratio. Furthermore, the result of iPP/(HDPE/CB) 40/60 with a high drawing ratio shows that a reversible conductivity was obtained during the cyclic tensile testing ($\varepsilon = 10\%$), but an irreversible conductivity makes the film fail during use at the applied ε values of up to 15%. This makes them good piezoresistive candidates for ε-sensing materials. Moreover, a simple structural model was proposed to describe the reversible and irreversible phenomena in the electrical resistance behavior of the iPP/HDPE/CB films under tensile loading. © 2014 Wiley Periodicals, Inc. J. Appl. Polym. Sci. **2014**, *131*, 40686.

KEYWORDS: composites; extrusion; films

Received 25 October 2013; accepted 6 March 2014
DOI: 10.1002/app.40686

INTRODUCTION

Carbon black (CB)-filled conductive polymer composites (CPCs), especially multiphase composites, have been aggressively investigated for more than half of a century because of the extraordinary properties of CB, the versatility of the polymeric materials, and the great promises that these materials hold as multifunctional materials in the area of electronics, actuators, and sensors.[1–3] In such a ternary composite, the conductive fillers can selectively reside in one of the polymer phases or along the interface.[4,5] Once a filler network is formed within the filler-rich phase and when the filler-rich phase is also continuous in the whole material (i.e., double percolation), the ternary composite becomes conductive. The conductivity of ternary CPCs strongly depends on the filler networks and phase morphology, which are controlled by the processing conditions. For the large-scale preparation of CPCs, the preferred method is melt processing, during which the polymer melts undergo strong shear. In a previous work about isotactic polypropylene (iPP)/high-density polyethylene (HDPE)/CB composites fabricated by melt processing,[6] it was found that the CB selectively distributed in the polyethylene phase, and a cocontinuous structure of the iPP phase and HDPE/CB phase was present in the composites. During the melt shear and flow in an extruder, the drops of the dispersed phase can be divided into small drops, and these small drops can be transformed into rods by melt-drawing. This may improve the continuity of the dispersed phase, and blends in the composites even may transform into a cocontinuous structure at appropriate composition ratios.

Polymer-based conductive films[7,8] have been shown to have favorable future because of their wide potential applications, such as in gas, chemistry, and strain (ε) sensors. Conventionally, it is accepted that special aligned conductive fillers in composites or a special phase morphology in the polymeric materials can provide a highly reversible ε-resistivity behavior.[9] Shin et al.[10] found that when the carbon nanotube forests formed in the matrix, a combination of high stretchability and high electrical conductivity was obtained in the polyurethane (PU)/multiwalled carbon nanotube film. These films provided highly

reversible stress (σ)–ε behavior and little degradation in the mechanical and electrical properties when they were stretched to 30% ε. Liu et al.[11] investigated the phase structure and mechanical behaviors of polypropylene hard elastic films. Lee et al.[12] studied the lamellar crystalline structure of hard elastic HDPE films. They all found that films fabricated by the extrusion casting method presented a highly oriented lamellar crystalline structure and provided a highly reversible σ–ε behavior.

In this study, CB was homogeneously dispersed in the HDPE matrix through twin-screw-extruder blending, and then, HDPE/CB was distributed in iPP. The extrusion casting method was used to produce the iPP/HDPE/CB conductive film. There were two intended purposes for this: (1) the formation of a continuous filler network in the HDPE phase and a cocontinuous structure of the iPP and HDPE/CB phases in the composites, which can ensure a good electrical conductivity of films, and (2) the generation of a stacked lamellar structure with a growing direction perpendicular to the extrusion direction in the matrix, which may bring about a novel mechanical performance for conductive films. The morphology and ε-sensing behavior of the films were investigated. Then, on the basis of this research, a simple structure model was proposed to describe the reversible and irreversible phenomena in the electrical resistance behavior of the iPP/HDPE/CB films under tensile loading. The unique mechanical and electrical properties of the composite films make them candidates for practical applications.

EXPERIMENTAL

Materials

CB (VXC-72, mean particle size = 30 nm, specific surface area = 254 m^2/g, and dibutyl phthalate absorption = 178 mL/100 g) was supplied by Cabot Corp. A commercial iPP (PPH, with a melt flow rate of 0.5 g/10 min, supplied by ExxonMobil) and a commercial HDPE (2911, melt flow rate = 20 g/10 min, supplied by Fushun Petroleum Chemical Co, Ltd., China) were used as the matrix materials.

Preparation of the iPP/HDPE/CB Conductive Films

The HDPE and CB particles (with a fixed mass ratio of HDPE to CB of 80:20) were melt-blended through a twin-screw extruder (SHJ-20, length-to-diameter ratio = 20, Nanjing Giant Machinery Co., Ltd.) with a temperature profile of 180, 200, 210, and 205°C from the hopper to die and a screw rotation of 120 rpm. The prepared HDPE/CB conductive composites (conductive phase) and pure iPP were pumped into the twin-screw extruder with a temperature profile of 180, 210, 225, and 215°C from the hopper to die and a screw rotation of 120 rpm to obtain the ternary composites. Finally, the iPP/HDPE/CB pellets pumped into a single-screw extruder equipped with a film die (SJ-20BX25) with a temperature profile of 180, 200, 220, and 215°C from the hopper to the die and a screw rotation of 30 rpm. Then, a series of iPP/HDPE/CB conductive films was prepared by the extrusion casting method with the draw ratio (the linear velocity of the rotation of the take-up roll divided by the velocity of the melt outflow from the die exit) from 1 to 16. However, films with high drawing ratios could not be obtained when the content of the conductive phase went beyond 60 wt %. The nanocomposite films were denoted as iPP/(HDPE/CB) x/y–z, where x, y, and z stand for the iPP content, the HDPE/CB content in the composites films, and the drawing ratio, respectively. Then, the prepared conductive films were cut into strips 10 mm wide by 20 mm long for the electrical resistivity measurement and cut into dumbbell-shaped specimens for tensile testing.

Characterization

An FEI Inspect F scanning electron microscope (Inspect F, FEI Co.) with an acceleration voltage of 20 kV was used to measure the phase and crystalline morphology of the conductive films. The film samples were fractured in liquid nitrogen, and the fracture surfaces were coated with gold for phase structure observation. The film specimens were surface-etched according to the permanganic etching technique described in ref. 13 for crystalline morphology observation. The resistance of the films was measured with a Keithley 6517B electrometer (Keithley Instruments, Inc., Ohio). Two-point method was used. Silver paint was applied to both ends of 2 mm long sample to ensure good contact. As a result, the contact resistance was negligible compared to the sample resistance. The bulk resistivity was calculated by eq. (1):

$$\rho = \frac{RS}{L} \tag{1}$$

where L, R, and S are the effective length, resistance, and cross-sectional area of the specimen, respectively. Then, the dumbbell-shaped specimens were used for tensile testing with a tensile test machine (AGS-J, Shimadzu Co., Japan) at room temperature. To ensure that the response of the conductive network changed synchronously with ε as much as possible, the specimens were stretched in tension quasi-statically at a rate of 1 mm/min. The ε of the film was recorded with a computer connected to the tensile test machine, whereas the resistance of the film was simultaneously measured with Keithley 6517B electrometer.

RESULTS AND DISCUSSION

Figure 1(a) shows the effects of the conductive phase (HDPE/CB) content on the resistivity of the nanocomposite films prepared at different drawing ratios. The resistivity of the films decreased with increasing conductive phase content but increased with increasing drawing ratio. The power law [eq. (2)] was used to analyze the resistivity of the nanocomposite films:[14]

$$\rho \propto \rho_0 (m - m_c)^{-t} \tag{2}$$

where ρ_0 is the bulk resistivity of the conductive phase, m is the mass fraction of the conductive phase, and t is the universal critical exponent, which depends on the dimensionality of the conductive network. The percolation threshold (m_c) is the critical content of the conductive particles, above which a continuous conductive network was formed for the transport of electrons throughout the matrix. Hence, we calculated that the m_c values were 39.0 and 46.4 wt % for the samples iPP/(HDPE/CB) x/y−3 and iPP/(HDPE/CB) x/y−10, respectively. This indicated that m_c increased with increasing drawing ratio. Furthermore, t of iPP/(HDPE/CB) x/y−3 and iPP/(HDPE/CB) x/y−10 were fitted, with calculated values of t of 1.67 and 1.47,

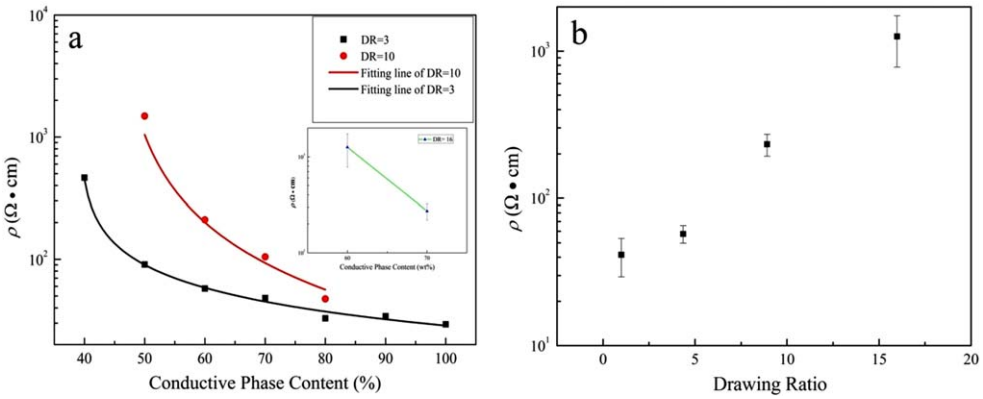

Figure 1. (a) Electrical resistivity (ρ) plotted against the conductive phase content of films with different drawing ratios (DRs). The solid lines are the fitting results from eq. (2), and the inset presents the electrical resistivity of iPP/(HDPE/CB) $x/y-16$. (b) Electrical resistivity of the iPP/(HDPE/CB) 40/60–z films as a function of the drawing ratio. [Color figure can be viewed in the online issue, which is available at wileyonlinelibrary.com.]

respectively. It indicated that a two-dimensional conductive network formed in the films.[15]

For the iPP/HDPE/CB conductive films, the composition ratios of the blend and drawing ratios were important factors in the final conductive properties. The film was insulative when the content of the conductive phase was lower than 40 wt %, whereas the film-forming ability was poor when the content of the conductive phase was higher than 70% [see the inset in Figure 1(a)]. To systematically research the extrusion casted film at different drawing ratios, the iPP/(HDPE/CB) 40/60–z films were selected as candidates for the morphological and electromechanical performance investigation when the conductive properties and forming abilities of the composites were considered. The electrical resistivity values of the iPP/(HDPE/CB) 40/60–z films plotted with drawing ratio are shown in Figure 1(b). They suggested that the electrical resistivity of the films increased with the drawing ratio.

Figure 2(a–c) shows the scanning electron microscopy (SEM) micrographs of the fracture surfaces of iPP/(HDPE/CB) 40/60–z. The black area is the iPP phase, and the light-colored area is the conductive phase. It was obvious that the conductive phase and iPP phase exhibited a cocontinuous structure in all of the film samples. When the drawing ratio increased, the elongated molten droplets of the conductive phase [Fig. 2(a)] experienced a large extensional deformation; this led to a reduction in the phase size and the improvement of the continuousness of the conductive phase [Fig. 2(b,c)]. In addition, the CB particles were observed in the HDPE phase, as shown in Figure 2(a, inset), because of the selective dispersion of CB particles in the iPP/HDPE blends.[6] Tabatabaei et al.[16] investigated the effect of processing on the crystalline orientation, morphology, and mechanical properties of the polypropylene cast films. Du et al.[17] studied the nanostructure and mechanical measurement of highly oriented lamellae of melt-drawn HDPE. They all found that the oriented lamellar crystalline structure formed in the matrix by melt drawing. The lamellar crystalline structure of iPP/(HDPE/CB) 40/60–z are shown in Figure 2(d–f). The randomly oriented lamellae formed in the matrix of the film were fabricated with a drawing ratio of 3 [Figure 2(d)]. With a drawing ratio up to 10, a certain oriented lamellar crystal with a growing direction perpendicular to the drawing direction began to present [Figure 2(e)]. When the drawing ratio increased to 16, a large of number of oriented lamellar crystals with a growing direction perpendicular to the drawing direction were formed in the matrix [Figure 2(f)]. This indicated that the drawing ratio had a positive effect on the orientation of the lamellar crystals.

The mechanical and piezoresistive tensile response of the conductive films is shown in Figure 3, where the film is loaded with quasi-static uniaxial tension up to the failure of electrical measurements. In Figure 3, σ (left vertical axis) and the normalized resistance (R/R_0; right vertical axis, where R_0 is the value of the electrical resistance before loading and R is the instantaneous resistance) are plotted against the applied ε. As shown in the σ versus ε plots, the iPP/(HDPE/CB) 40/60–1 film showed brittle fracture behavior with an average ultimate ε of 12% [Figure 3(a)]. The composite films exhibited excellent toughness with increasing drawing ratio [Figure 3(b–d)]. The evaluative sensing (gauge) factor, which measures the ε sensitivity of the conductive network, is defined as the ratio of the relative resistance change to the mechanical ε [$K=(\Delta R/R_0)/\varepsilon$, where K stands for the gauge factor.]. The mechanical behaviors correlated with the piezoresistive (R/R_0 vs ε) curves and gauge factors are presented in Figure 3. As shown in Figure 3, a linear piezoresistivity was obtained in the elastic regime until the ε value was up to the yield point of the films [except in the sample iPP/(HDPE/CB) 40/60–1]. With further increases in ε, the resistance change of the composite films passed a point of inflexion, and this was followed by a drastic increase shortly before the final failure of the electrical properties. This could be explained by the fact that the resistivity of a given polymer/filler system is dictated by the number of contact points of the conductive network and the distances between the neighboring particles.[18] Furthermore, the gauge factor of the films within the elastic region decreased with increasing drawing ratio, as shown in Figure 3. This suggested that the sensitivity of the ε gauge of the films decreased with increasing drawing ratio.

For the oriented lamellar crystalline structure and excellent electrical properties, the iPP/(HDPE/CB) 40/60–16 films were

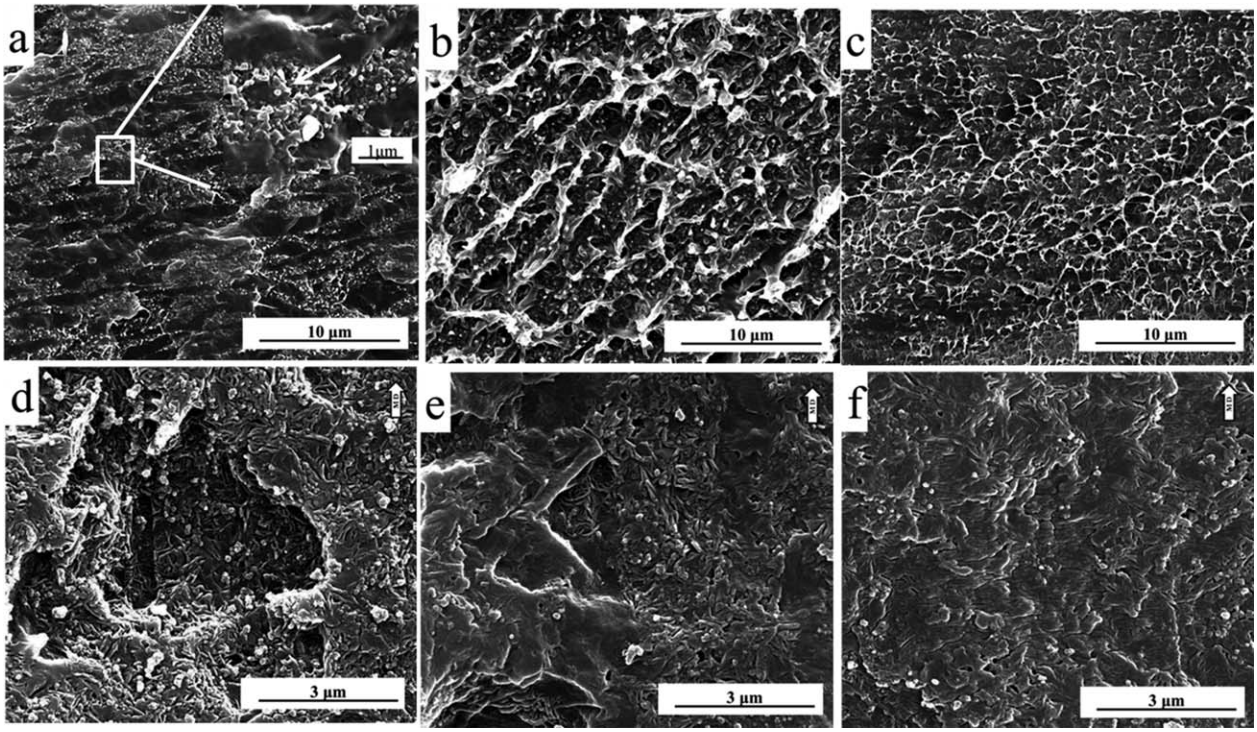

Figure 2. SEM micrographs of the fracture surfaces of iPP/(HDPE/CB) 40/60–*z* [(a) $z = 3$, (b) $z = 10$, and (c) $z = 16$] and the crystalline morphology of iPP/(HDPE/CB) 40/60–*z* [(d) $z = 3$, (e) $z = 10$, and (f) $z = 16$]. MD = melt-drawn direction. The inset is a local magnification image of the fracture of iPP/(HDPE/CB) 40/60–3.

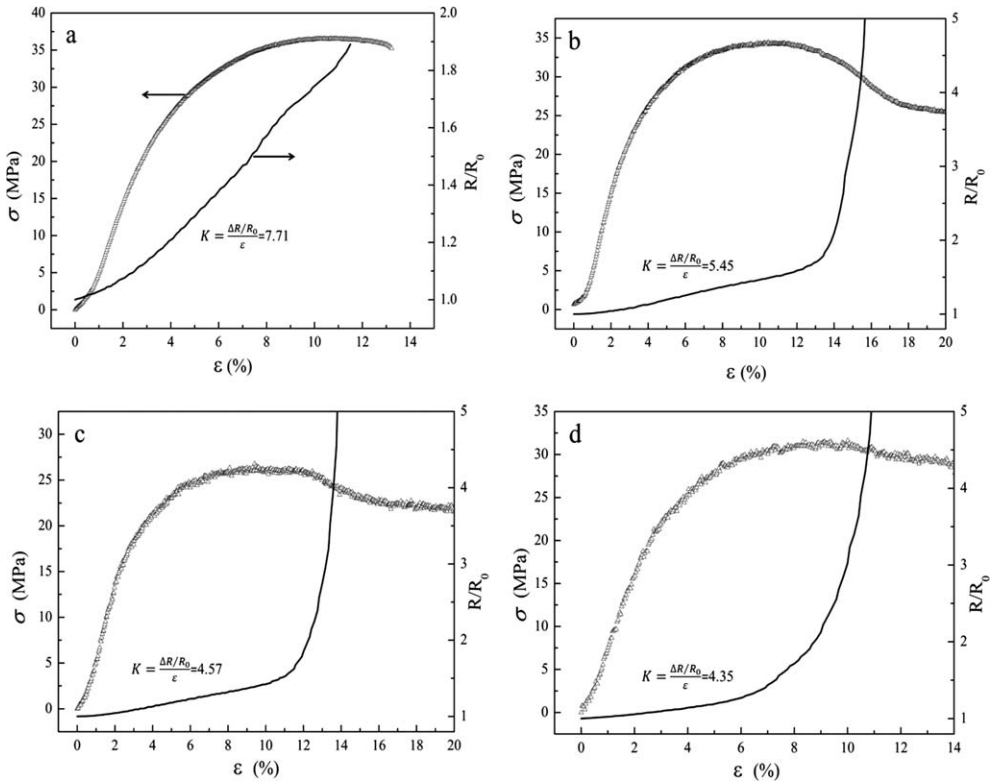

Figure 3. Tensile σ (left vertical axis) and R/R_0 (right vertical axis) versus ε for iPP/(HDPE/CB) 40/60–*z*: (a) $z = 1$, (b) $z = 3$, (c) $z = 10$, and (d) $z = 16$.

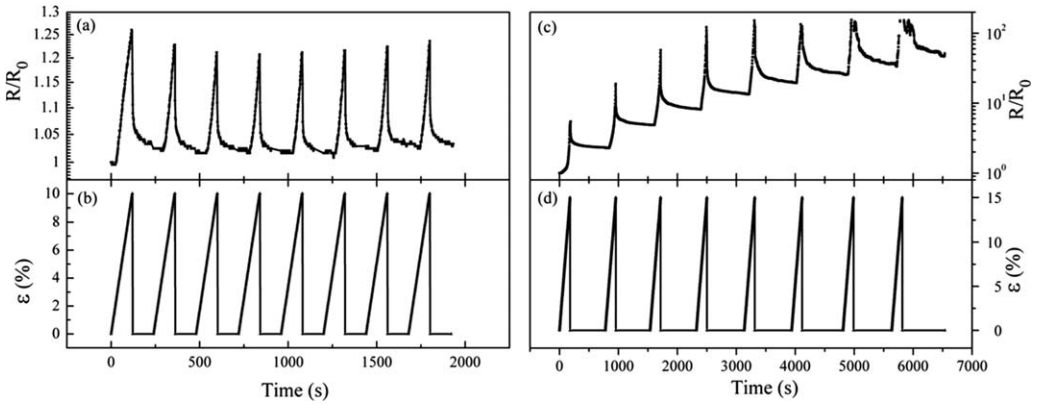

Figure 4. (a,c) Piezoresistive variations (R/R_0) of iPP/(HDPE/CB) 40/60–16 with different ε levels and (b,d) cyclic deformations (elongation of the film).

subjected to cycle tensile testing for the investigation of the ε-sensing behavior. The response of R/R_0 to ε during cycle tensile testing is shown in Figure 4. As the ε value was set at 10% (in the vicinity of the yield point), the electrical behavior as a function of time and correlated to ε is plotted in Figure 4(a,b), with the normalized electrical resistance reproducing the time evolution of ε. This provided a hint that the conductive network could recover to a perfect state with an R/R_0 equal to the initial value of the sample after the external force was removed completely at this ε level. However, with a total ε value of up to 15% (beyond the yield point) during every cycle, the conductive films exhibited a different behavior during the deformation, as shown in Figure 4(c,d). Although the cycling behavior of R/R_0 at this ε level followed a similar pattern for each loading cycle, the numerical values attained by R/R_0 were quite different. There was a marked growth of amplitude of R/R_0 as the number of cycles increased, and the ongoing extension cycles had a contributing effect on the residual normalized electrical resistance. This suggested that part of the network structure was permanently damaged when the ε value of the film was up to 15%. The good repeatability and linearity between the resistivity change and ε within the elastic region were advantages for piezoresistive ε sensor applications. Furthermore, the step-up amplitude of R/R_0 within the relatively high deformation level could be used in a safety monitoring material. This kind of conductive film could be selected as a potential candidate for ε-sensing materials.

The mechanism of the diversified variation in the resistance of the films probably combined several effects. We observed that the lamellar crystalline structure played an important role in the recovery of the conductive network and the extended elastic regime of the film under tension. A simplified model was used to explain the movement of the lamellar crystalline structure during loading and unloading and was built for the reversible and irreversible phenomena in the normalized electrical resistance behavior of iPP/(HDPE/CB) 40/60 (shown in Figure 5). The chains between the lamellae and amorphous regions were straightened, and the oriented lamellae slipped or separated with the applied ε. At the same time, the distances between the neighboring particles increased, and the number of the effective conductive paths decreased with the straightening of the chains and the separation of an oriented lamellar. With the removal of the external force, the lamellae could recover to their initial state because of movement of the noncrystalline chains.[19–21] The recovery of the oriented lamellae drove the particle network back to the original position. The CB aggregates moved apart with the movement of lamellae during loading. Then, the CB particles reaggregated with the recoverable lamellae during unloading. The irreversible behavior of the network structure of the film subjected to a ε of 15% is shown in Figure 5(b). After the removal of the external force, the noncrystalline chains could not recovery because of the broken noncrystalline chains under a 15% ε level. Moreover, the breakdown of the noncrystalline chains was accumulated with the number of cycles. The lamellae and CB aggregates presented similar behavior. So the large ε level caused a significant unrecoverable breakdown of the CB agglomerates and lamellae. Furthermore, with increasing number of cycles, the extreme of resistance was elevated as well. This indicated that the unrecoverable breakdown of the CB agglomerates and lamellae was more and more serious with the increasing number of cycles.

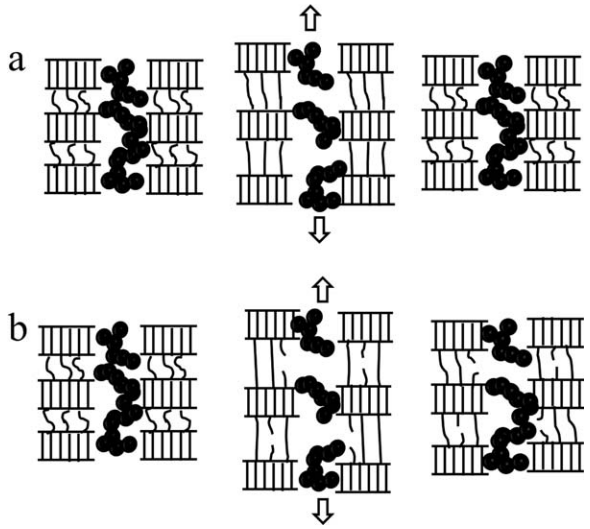

Figure 5. Schematics of the movement of the CB aggregates and lamellae during the cycle test at different ε levels: (a) 10 and (b) 15%.

CONCLUSIONS

In this study, cast film extrusion, an easy and feasible method, was used to fabricate a novel conductive thin film on the basis of the blending of iPP, HDPE, and CB. The electrical resistivity and m_c increased with increasing drawing ratio. Moreover, the SEM images showed that cocontinuous structures formed in the films, and the drawing ratio had a positive effect on the orientation of the lamellar crystals. The gauge factor of the films within the elastic region decreased with increasing drawing ratio. What is more, the electromechanical tests showed that a reversibly conductivity was obtained during the cyclic tensile testing at a ε of 10%, but an irreversibly conductivity was obtained when the ε value was up to 15%. This makes them good piezoresistive candidates for ε-sensing materials. Then, a simplified structure model to explain the reversibility and irreversibility of the electrical resistance of the composite films during cycle tensile was developed.

ACKNOWLEDGMENTS

This research was supported by the National Natural Science Foundation of China (contract grant number 51103087). The authors acknowledge Chaoliang Zhang (West China College of Stomatology, Sichuan University) for the SEM observations.

REFERENCES

1. Zee, F.; Judy, J. W. *Sens. Actuators B* **2001**, *72*, 120.
2. Lonergan, M. C.; Severin, E. J.; Doleman, B. J.; Beaber, S. A.; Grubbs, R. H.; Lewis, N. S. *Chem. Mater.* **1996**, *8*, 2298.
3. Knite, M.; Teteris, V.; Kiploka, A.; Kaupuzs, J. *Sens. Actuators A* **2004**, *110*, 142.
4. Wichmann, M. H. G.; Buschhorn, S. T.; Gehrmann, J.; Schulte, K. *Phys. Rev. B* **2009**, *80*, 5437.
5. Gubbels, F.; Jérôme, R.; Teyssie, P.; Vanlathem, E. *Macromolecules* **1994**, *27*, 1972.
6. Yin, C. L.; Liu, Z. Y.; Gao, Y. G.; Yang, M. B. *Polym. Adv. Technol.* **2012**, *23*, 1112.
7. Aguilar, J. O.; Bautista-Quijano, J. R.; Avilés, F. *Exp. Polym. Lett.* **2010**, *4*, 292.
8. Baltopoulos, A.; Athanasopoulos, N.; Fotiou, I.; Vavouliotis, A.; Kostopoulos, V. *Exp. Polym. Lett.* **2013**, *7*, 40.
9. Rein, M. D.; Breuer, O.; Wagner, H. D. *Compos. Sci. Technol.* **2011**, *71*, 373.
10. Shin, M. K.; Oh, J.; Lima, M.; Kozlov, M. E.; Kim, S. J.; Baughman, R. H. *Adv. Mater.* **2010**, *22*, 2663.
11. Liu, D.; Kang, J.; Xiang, M.; Cao, Y. *J. Polym. Res.* **2013**, *20*, 1.
12. Lee, S. Y.; Park, S. Y.; Song, H. S. *Polymer* **2006**, *47*, 3540.
13. Wang, L.; Yang, B.; Yang, W.; Sun, N.; Yin, B.; Feng, J. M.; Yang, M. B. *Colloid Polym. Sci.* **2011**, *289*, 1661.
14. Zhou, T. N.; Qi, X. D.; Fu, Q. *Express Polym. Lett.* **2013**, *7*, 747.
15. Bauhofer, W.; Kovacs, J. Z. *Compos. Sci. Technol.* **2009**, *69*, 1486.
16. Tabatabaei, S. H.; Carreau, P. V. J.; Ajji, A. *Polymer* **2009**, *50*, 4228.
17. Du, B.; Zhang, J.; Zhang, Q. *Macromolecules* **2000**, *33*, 7521.
18. Pham, G. T.; Park, Y. B.; Liang, Z.; Zhang, C.; Wang, B. *Compos. B* **2008**, *39*, 209.
19. Samuels, R. J. *J. Macromol. Sci. Phys.* **1973**, *8*, 41.
20. Ding, Z. T.; Bao, R. Y.; Zhao, B.; Yan, J.; Liu, Z. Y.; Yang, M. B. *J. Appl. Polym. Sci.* **2013**, *130*, 1659.
21. Song, Y.; Nitta, K.; Nemoto, N. *Macromolecules* **2003**, *36*, 1955.